CHINESE OPTICS LETTERS

Vol. 20, No. 7 | July 2022

Automatic, long-term frequency-stabilized lasers with sub-hertz linewidth and 10^{-16} frequency instability

Chengzhi Yan (晏城志), Haosen Shi (师浩森)*, Yuan Yao (姚 远), Hongfu Yu (于洪浮), Yanyi Jiang (蒋燕义)**, and Longsheng Ma (马龙生)

State Key Laboratory of Precision Spectroscopy, East China Normal University, Shanghai 200062, China

*Corresponding author: hsshi@lps.ecnu.edu.cn

**Corresponding author: yyjiang@phy.ecnu.edu.cn

Received March 18, 2022 | Accepted April 24, 2022 | Posted Online May 26, 2022

We report two ultra-stable laser systems automatically frequency-stabilized to two high-finesse optical cavities. By employing analog-digital hybrid proportional integral derivative (PID) controllers, we keep the merits of wide servo bandwidth and servo accuracy by using analog circuits for the PID controller, and, at the same time, we realize automatic laser frequency locking by introducing digital logic into the PID controller. The lasers can be automatically frequency-stabilized to their reference cavities, and it can be relocked in 0.3 s when interruption happens, i.e., blocking and unblocking the laser light. These automatic frequency-stabilized lasers are measured to have a frequency instability of 6×10^{-16} at 1 s averaging time and a most probable linewidth of 0.3 Hz. The laser systems were tested for continuous operation over 11 days. Such ultra-stable laser systems in long-term robust operation will be beneficial to the applications of optical atomic clocks and precision measurement based on frequency-stabilized lasers.

Keywords: narrow-linewidth laser; automatic frequency stabilization; optical atomic clock; gravitational wave detection.
DOI: 10.3788/COL202220.070201

1. Introduction

Lasers with high-frequency stability and narrow linewidth are indispensable tools in optical atomic clocks[1,2], gravitational wave detection[3], low noise optical/microwave synthesis[4,5], tests of fundamental physics, and precision measurement[6,7]. Such lasers are usually achieved by locking the laser frequency to the resonance of ultra-stable Fabry–Pérot cavities with the Pound–Drever–Hall (PDH) technique[8]. To realize the aforementioned applications, many labs around the world have constructed ultra-stable lasers with frequency instabilities at the 10^{-16} level[2,9–14]. Some have constructed lasers with frequency instabilities of 10^{-17}, which are stabilized to cryogenic cavities[15,16] or optical cavities at room temperature with a length larger than 35 cm[17] for lower cavity thermal noise[18]. While methods for further improving laser frequency stability and laser linewidth are explored[19,20], there is growing interest in making such frequency-stabilized laser systems transportable[12,13,21–24], automated, robust, and suitable for practical applications[25,26].

In terms of long-term robust operation, some of the ultra-stable laser systems have achieved a continuous operation time for more than 10 days with analog proportional integral derivative (PID) controllers[27]. Those lasers were tested in a quiet room. However, in case of interruption, those lasers will lose frequency locking, and they need to be relocked by hand. Therefore, it is beneficial to introduce automatic frequency locking and relocking in such laser systems for long-term robust operation. Moreover, automatic frequency stabilization is crucial to some unmanned applications, i.e., space-borne scientific missions[28,29]. It also provides convenience for complicated systems containing several stable lasers, i.e., optical atomic clocks.

To achieve automatic frequency locking and relocking, digital control is usually employed[7,30,31]. In an automatic frequency-locking, cavity-stabilized laser system, the PDH signal or the cavity transmission signal is digitized for determining the frequency matching between the laser and the cavity resonance and for monitoring the locking state as well. A digital-controlled laser frequency scan is also employed to set the laser frequency close to the cavity resonance. Hence, analog to digital converters (ADCs) and digital to analog converters (DACs) are commonly used to bridge the analog signals and the digital logic.

However, in servo systems (also called PID controller or loop filter), there are two ways in dealing with the error signal for correcting the laser frequency. Either an all-digital PID controller[7,30] or an analog-digital hybrid PID controller[32] is chosen. When using an all-digital PID controller, i.e., that based on field programmable gate arrays (FPGAs), the PDH signal (the error

signal) is digitalized, processed by digital PID algorithms, and then converted back to an analog signal to control the laser frequency actuator[33]. The resolution of ADCs and DACs determines the noise level feeding to the actuator, while their conversion rate and bandwidth determine feedback response time. Since the resolution and conversion rate of ADCs and DACs cannot be satisfied at the same time, one has to make a tradeoff between the laser frequency feedback bandwidth and the laser frequency stability. A frequency-stabilized Nd:$Y_3Al_5O_{12}$ (Nd:YAG) laser based on an all-digital PID controller is demonstrated with a frequency instability of 1×10^{-15} at 1 s averaging time[7]. When using an analog-digital hybrid PID controller, the PDH signal is processed in analog circuits, and then it is directly fed to the laser frequency actuator, while digital logic controls the analog PID values. Laser systems based on analog-digital hybrid PID controllers have merits of both high laser frequency feedback bandwidth and laser frequency control accuracy. Based on an analog-digital hybrid PID controller, an automatic frequency-locking, external-cavity diode laser system is realized, which has a linewidth of 3 Hz[32].

In this Letter, we use analog-digital hybrid PID controllers to realize automatic laser frequency locking while enjoying the merits of wide servo bandwidth and high servo accuracy. Two Nd:YAG lasers are automatically frequency-stabilized to the resonance of two high-finesse, transportable optical cavities with the help of analog-digital hybrid PID controllers. The laser frequency can be locked over more than 11 days, and it can be relocked in 0.3 s when perturbations break laser frequency locking. By frequency comparison, each laser is measured to have a frequency instability of 6×10^{-16} at 1 s averaging time and a most probable linewidth of 0.3 Hz. Such kind of ultra-stable lasers in a long-term robust operation are urgently needed in the applications of today's optical atomic clocks when making long-term frequency comparisons and as a secondary frequency standard. Meanwhile, such automatic frequency-stabilized lasers are suitable for scientific missions in space.

2. Experimental Setup

The experimental setup for laser frequency stabilization is shown in Fig. 1. It is similar to our previous work[24] except for the analog-digital hybrid PID controller. The light from a Nd:YAG laser at 1064 nm is split into several parts for laser frequency stabilization and performance evaluation (not shown in the figure). In each part, the laser light is coupled into a piece of polarization maintaining (PM) optical fiber for being delivered to a reference cavity or measurement setup. Fiber noise cancellation (FNC)[34] is employed to remove random phase/frequency noise induced by the optical fibers.

In the setup of laser frequency stabilization, the laser light output from the PM fiber is frequency-shifted by an acoustic-optic modulator (AOM). The driving power of the AOM is adjusted for light power stabilization by monitoring the voltage from a photo-detector (PD_1). Then, the diffraction laser light from the AOM passes through a polarizer (P_1), and it is phase-modulated

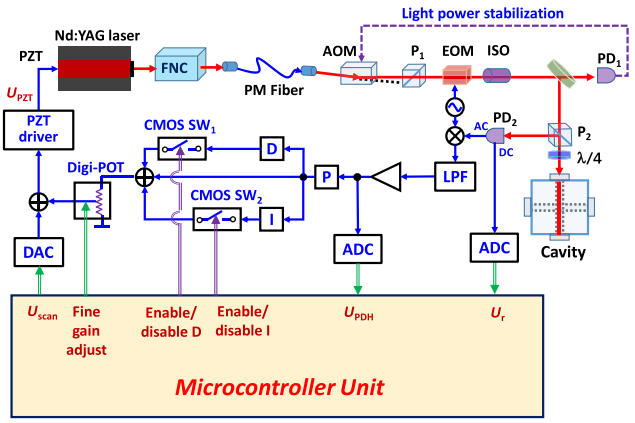

Fig. 1. Schematic diagram of the experimental setup for automatic laser frequency stabilization based on an analog-digital hybrid PID controller. FNC, fiber noise cancellation; PM fiber, polarization maintaining optical fiber; AOM, acousto-optic modulator; P_1 and P_2, polarizers; EOM, electro-optic modulator; ISO, optical isolator; $\lambda/4$, quarter-wave plate; PD, photo-detector; LPF, low pass filter; ADC, analog to digital converter; CMOS SW, CMOS analog switch; Digi-POT, digital potentiometer; PZT, piezo transducer.

at the modulation frequency of $f_{\mathrm{mod}} \sim 4.1$ MHz in an electro-optic modulator (EOM). To reduce residual amplitude modulation, an optical isolator (ISO) is placed after the EOM to prevent any light being reflected back into the EOM. Then, the modulated light is coupled to a 10-cm-long optical cavity, which has a finesse of ~700,000 and a cavity reflection contrast of 40%. The cavity reflection light is steered onto PD_2. The AC output of PD_2 is demodulated in a double balanced mixer (DBM), and then it is filtered in a low pass filter (LPF) to generate a PDH-based frequency discrimination signal for laser frequency stabilization. The PDH signal is sent to an analog-digital hybrid PID controller, and then the output together with an offset voltage is amplified by a high-voltage driver (U_{PZT}) to feedback to a piezo transducer (PZT) inside the laser cavity to control the laser frequency. After closing the servo loop, the servo bandwidth is ~80 kHz, limited by the response time of the PZT.

In the analog-digital hybrid PID controller, the amplified PDH signal is converted to a digital signal (U_{PDH}) by a 12 bit ADC inside the microcontroller unit (MCU, STM32F407) with a sampling rate of 1 MSa/s. Another ADC inside the MCU samples the DC output of PD_2 (cavity reflection light power) as U_{r}. A separate 18 bit DAC is used to control the temperature of the laser crystal to make the laser frequency close to a desired value by reading the laser frequency on a wavemeter with an uncertainty of ±60 MHz (not shown in the figure). There is a second 18 bit DAC to generate an analog voltage (U_{scan}) for laser frequency scan via the PZT. In the current design, the laser frequency scan range by adjusting the PZT is ~200 MHz. Therefore, each frequency step is $\nu_{\mathrm{stp}} = 200\ \mathrm{MHz}/2^{18} \sim 760$ Hz. Comparing with the cavity linewidth of 2.1 kHz, it is sufficient to capture the signal of U_{PDH} and U_{r} when the light frequency is scanned across the cavity resonance. As long as the laser frequency is close to the cavity resonance, the MCU sends

commands to turn on complementary metal oxide semiconductor (CMOS) analog switches (SWs) to enable integration (I) and differentiation (D). The values of capacitances for I and D are pre-optimized. A digital potentiometer (Digi-POT, AD7376) sets the fine gain (P) of the PID to optimize the feedback loop.

3. Methods and Results

The logical block diagram of automatic laser frequency locking is shown in Fig. 2(a). Firstly, we set the values of $U_{\mathrm{PDH-0}}$ and $U_{\mathrm{r-0}}$, which are used to determine whether the laser frequency is close to the cavity resonance and the status of laser frequency locking according to the voltage of the PDH signal and the cavity

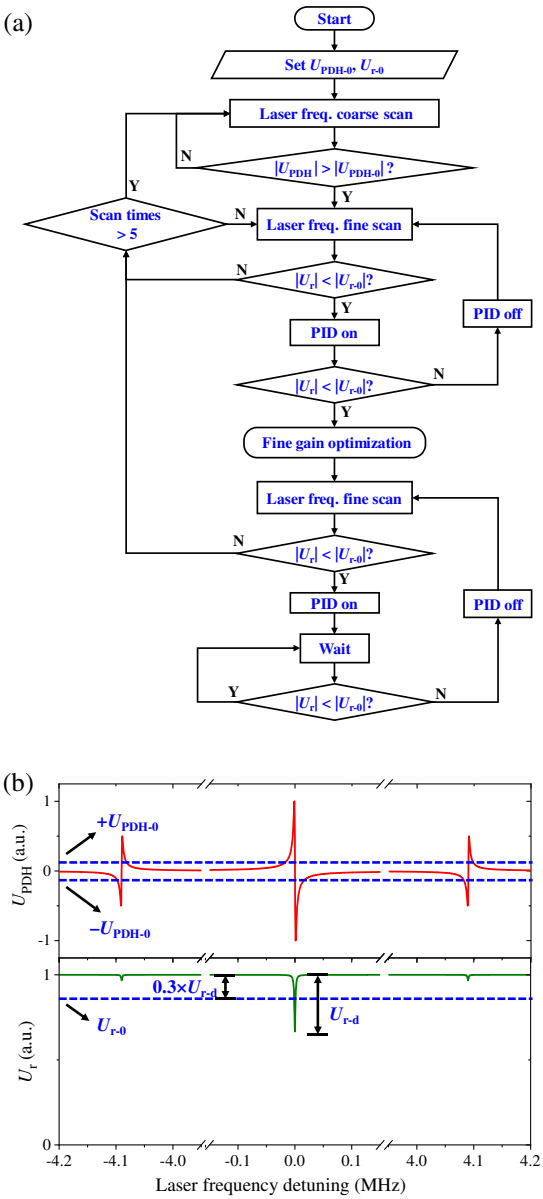

Fig. 2. (a) Logic block diagram of automatic laser frequency locking. (b) The PDH signal and the cavity reflection signal with $U_{\mathrm{PDH-0}}$ and $U_{\mathrm{r-0}}$ marked.

reflection light power. The value of $U_{\mathrm{PDH-0}}$ is set to ~10 times larger than the noise level of the PDH signal, and the value of $U_{\mathrm{r-0}}$ is set to ~30% of the reflection dip ($U_{\mathrm{r-d}}$), as shown in Fig. 2(b).

The locking process can be separated into five phases. In Phase I, the laser frequency is coarsely scanned by a step of $32 \times \nu_{\mathrm{stp}} \sim 24$ kHz. The time for the full coarse scan is ~90 ms, with 2^{13} steps in total and a single step time of 10 μs. As long as $|U_{\mathrm{PDH}}| > |U_{\mathrm{PDH-0}}|$, the laser carrier or one of the sidebands is close to the cavity resonance, and then it stops the laser frequency coarse scan. The value of U_{scan} in this scan step is recorded. With such a coarse step, we can quickly set the laser frequency close to the cavity resonance with a certainty of $\pm f_{\mathrm{mod}}$ by monitoring U_{PDH}.

In Phase II, the laser frequency is finely scanned with a frequency step of $\nu_{\mathrm{stp}} \sim 760$ Hz. The fine scan range is $\sim 3 \times f_{\mathrm{mod}}$, centered at the point when $|U_{\mathrm{PDH}}| > |U_{\mathrm{PDH-0}}|$. It takes 160 ms to make a full fine frequency scan. As long as $|U_{\mathrm{r}}| < |U_{\mathrm{r-0}}|$, the laser carrier is close to the cavity resonance. Then, in Phase III, MCU enables D and I by turning on CMOS SW_1 and CMOS SW_2, accordingly. The resistance (R) value of the Digi-POT remains at the maximum value as that in Phases I and II. After that, the R of Digi-POT is optimized by monitoring U_{r}. The minimum mean value of U_{r} is found at R_{i}, which is recorded as the optimized fine gain. In Phase IV, it disables D and I by turning off CMOS SW_1 and SW_2 while Digi-POT is set to R_{i}. Then, the laser frequency is finely scanned again from the same point as that in the first fine scan. As long as $|U_{\mathrm{r}}| < |U_{\mathrm{r-0}}|$, CMOS SW_1 and CMOS SW_2 are turned on again, and Digi-POT is kept at R_{i}. In phase V, the laser is in locking, and U_{r} is monitored to check the status of laser locking.

Figure 3(a) shows the recorded U_{PZT}, U_{PDH}, and U_{r} in each phase of the automatic laser frequency locking. From 0 s to 0.05 s (Phase I), the laser frequency is coarsely scanned. At 0.05 s, $|U_{\mathrm{PDH}}| > |U_{\mathrm{PDH-0}}|$, then the MCU stops the coarse frequency scan and starts the fine frequency scan (Phase II). At ~0.12 s, although there is a peak on U_{PDH} as one of the laser sidebands resonant on the cavity, $|U_{\mathrm{r}}|$ is still larger than $|U_{\mathrm{r-0}}|$. Therefore, it continues to scan the laser frequency until $|U_{\mathrm{r}}| < |U_{\mathrm{r-0}}|$ at ~0.16 s. During 0.16 s to 0.35 s (Phase III), the fine gain is optimized by adjusting the R of the Digi-POT and monitoring U_{r}. In 0.35–0.45 s (Phase IV), the laser frequency is finely scanned again. At 0.45 s, the laser frequency is relocked to the cavity with the optimized fine gain. It takes ~0.5 s to lock the laser frequency to the cavity resonance.

We tested laser frequency relocking capability by blocking for 5 ms and unblocking the laser light. It is realized by turning off and on the driving signal of the AOM. We tested it for more than 10^4 times. Every time the laser frequency can be relocked to the cavity. Figure 3(b) shows the statistics of the relocking time. For more than 97% of the measurements, it takes less than 0.15 s to relock the laser frequency. For all the measurements, the laser frequency can be relocked in 0.3 s. Such a short relocking time benefits from the combination of the coarse and fine frequency scans.

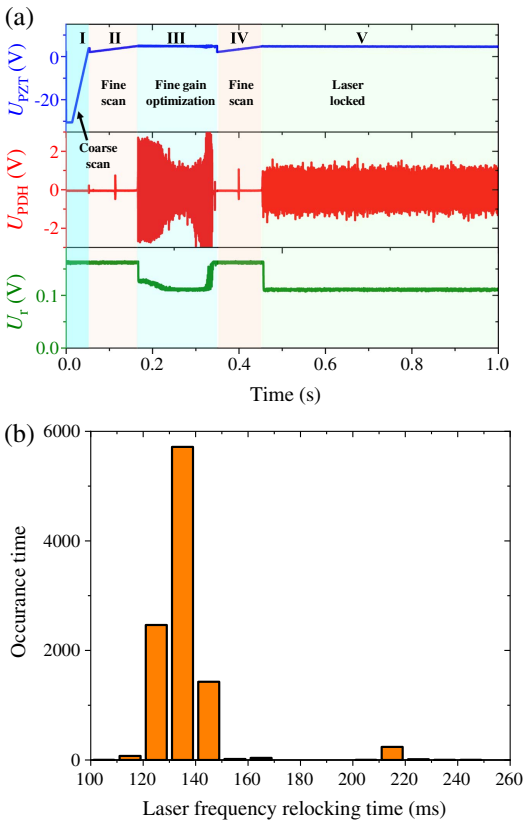

Fig. 3. (a) Signal of U_{PZT}, U_{PDH}, and U_r when the laser frequency starts to lock. (b) Statistics of laser frequency relocking time.

To characterize the performance of the automatic laser frequency stabilization system, we build two similar laser systems, which are separately stabilized to two reference cavities on the same spacer[24]. We measured the frequency as well as the spectrum of the beating signal between the laser systems. In Fig. 4(a), the beating frequency is recorded over 22 days. One laser (#1) lost frequency locking on the 11th and 15th days. On the 17th day, the computer that was monitoring the laser locking state by connecting with the MCUs and a frequency counter broke down. Both lasers lost frequency locking, probably due to an electrical shock onto the MCUs. In fact, for a normal operation, there is no need to connect the MCUs to the computer. From this measurement, we find that the lasers lost frequency locking mostly due to environmental disturbance, i.e., hard knock on the reference cavities and the lasers. During the 1st–11th days, when there are few environmental disturbances, the laser systems were continuously frequency-stabilized. The second laser kept continuous frequency locking for 17 days.

After deleting the data points when the lasers lost frequency locking, we calculate the Allan deviation of the beating frequency, which is shown in Fig. 4(b) with blue dots. The frequency instability of the beat note reaches 8.1×10^{-16} at 1 s averaging time. Assuming two laser systems have low correlation[24], each laser has a frequency instability of 6×10^{-16} at 1 s averaging time. If we split the whole dataset into four sub-datasets separated by the events of laser frequency unlocking, the Allan deviation of each sub-dataset is shown in the inset

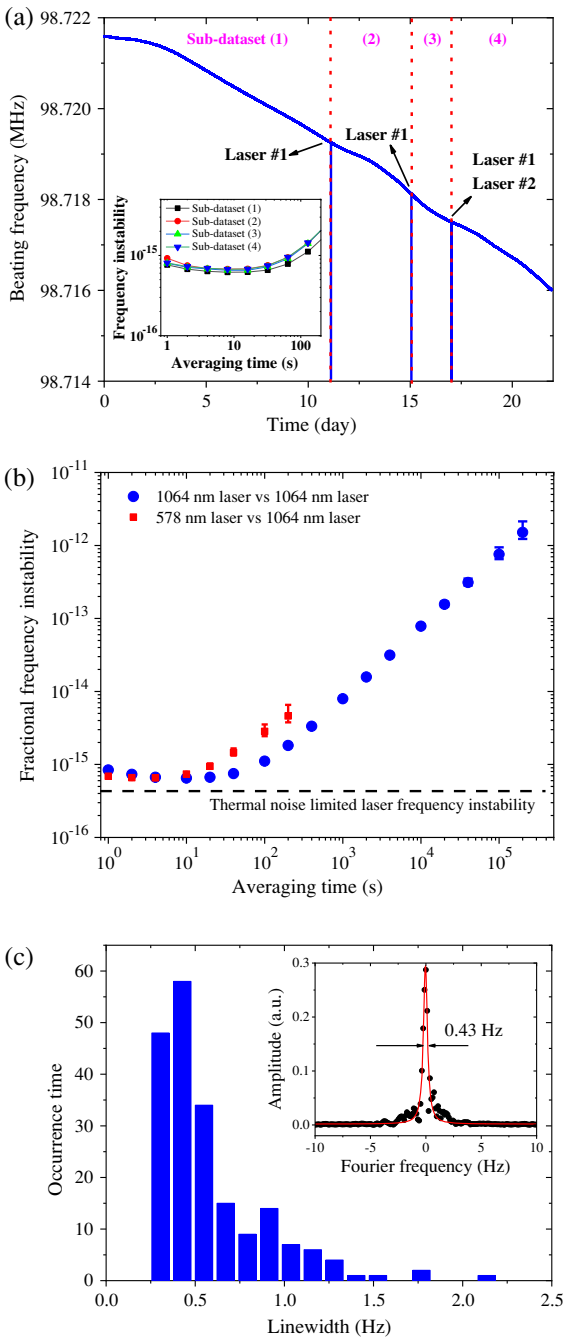

Fig. 4. (a) Recorded beating frequency between two automatic frequency-locking laser systems at 1064 nm over 22 days. The inset shows the frequency instability of four sub-datasets. (b) The frequency instability of the beat note between two automatic frequency-locking laser systems at 1064 nm (Lasers #1 and #2, blue dots) and between Laser #1 and a cavity-stabilized 578 nm laser (red squares). The black dashed line indicates the thermal noise-limited laser frequency instability for a single 1064 nm laser. (c) Distribution of the linewidth measurement of the beat note between Lasers #1 and #2 measured on an FFT spectrum analyzer with a resolution bandwidth of 122 mHz. The inset shows one of the measurements.

of Fig. 4(a). In each sub-dataset, the frequency instability at 1 s averaging time is 7.6×10^{-16}, 9.2×10^{-16}, 8.0×10^{-16}, and 8.1×10^{-16}, respectively. From this measurement, we can learn

that the frequency stability of the laser system will be better when there is less human activity and there is a negligible difference after automatic relocking.

We also measured the frequency instability of the automatic frequency-locking laser system at 1064 nm (#1) by comparing it against a cavity-stabilized laser at 578 nm via an optical frequency comb[35,36]. The frequency instability of the beat note between them is 6.9×10^{-16} at 1 s averaging time, as shown with the red squares in Fig. 4(b). Since the 578 nm laser has a frequency instability of 3.5×10^{-16} at 1 s averaging time during the daytime[14], the frequency instability of the 1064 nm laser (#1) is about 6×10^{-16} at 1 s averaging time. The laser frequency instability achieved in this paper is similar to those using traditional analog PID controllers[24], which is also close to the thermal noise-limited laser frequency stability of 4.3×10^{-16} (black dashed line).

We recorded the spectrum of the beat note between two 1064 nm cavity-stabilized lasers on a fast Fourier transform (FFT) spectrum analyzer with a resolution bandwidth of 122 mHz. By fitting each spectrum, we obtain the linewidth of the beat note. The inset of Fig. 4(c) shows one of the linewidth measurements. The distribution of the measured laser linewidth is shown in Fig. 4(c). The most probable linewidth is 0.45 Hz. Therefore, each laser has a probable linewidth of 0.3 Hz, assuming the laser systems have low correlation.

4. Conclusion

We demonstrate two automatic frequency-locking laser systems based on analog-digital hybrid PID controllers. The laser frequency can be automatically locked to its reference cavity, and it can be relocked in 0.3 s when there is a disturbance. Each laser system is measured to have a frequency instability of 6×10^{-16} at 1 s averaging time and a most probable linewidth of 0.3 Hz. The automatic frequency-locking scheme described in this paper provides a solution for ultra-stable lasers stabilized to high-finesse cavities for applications in optical atomic clocks and scientific missions in space.

Acknowledgement

This work was supported by the National Natural Science Foundation of China (No. 11927810).

References

1. A. D. Ludlow, M. M. Boyd, J. Ye, E. Peik, and P. O. Schmidt, "Optical atomic clocks," Rev. Mod. Phys. **87**, 637 (2015).
2. Y. Li, Y. Lin, Q. Wang, T. Yang, Z. Sun, E. Zang, and Z. Fang, "An improved strontium lattice clock with 10–16 level laser frequency stabilization," Chin. Opt. Lett. **16**, 051402 (2018).
3. B. Willke, K. Danzmann, M. Frede, P. King, D. Kracht, P. Kwee, O. Puncken, R. L. Savage, B. Schulz, F. Seifert, C. Veltkamp, S. Wagner, P. Webels, and L. Winkelmann, "Stabilized lasers for advanced gravitational wave detectors," Class. Quantum Grav. **25**, 114040 (2008).
4. Y. Yao, Y. Jiang, L. Wu, H. Yu, Z. Bi, and L. Ma, "A low noise optical frequency synthesizer at 700–990 nm," Appl. Phys. Lett. **109**, 131102 (2016).
5. T. M. Fortier, M. S. Kirchner, F. Quinlan, J. Taylor, J. C. Bergquist, T. Rosenband, N. Lemke, A. Ludlow, Y. Jiang, C. W. Oates, and S. A. Diddams, "Generation of ultrastable microwaves via optical frequency division," Nat. Photonics **5**, 425 (2011).
6. S. Herrmann, A. Senger, K. Möhle, M. Nagel, E. V. Kovalchuk, and A. Peters, "Rotating optical cavity experiment testing Lorentz invariance at the 10^{-17} level," Phys. Rev. D **80**, 105011 (2009).
7. F. Zhang, K. Liu, Z. Li, F. Cheng, X. Feng, K. Li, Z. Lu, and J. Zhang, "Long-term digital frequency-stabilized laser source for large-scale passive laser gyroscopes," Rev. Sci. Instrum. **91**, 013001 (2020).
8. R. W. P. Drever, J. L. Hall, F. V. Kowalski, J. Hough, G. M. Ford, A. J. Munley, and H. Ward, "Laser phase and frequency stabilization using an optical resonator," Appl. Phys. B **31**, 97 (1983).
9. B. C. Young, F. C. Cruz, W. M. Itano, and J. C. Bergquist, "Visible lasers with subhertz linewidths," Phys. Rev. Lett. **82**, 3799 (1999).
10. Y. Y. Jiang, A. D. Ludlow, N. D. Lemke, R. W. Fox, J. A. Sherman, L.-S. Ma, and C. W. Oates, "Making optical atomic clocks more stable with 10^{-16}-level laser stabilization," Nat. Photonics **5**, 158 (2011).
11. B. Argence, E. Prevost, T. Lévèque, R. Le Goff, S. Bize, P. Lemonde, and G. Santarelli, "Prototype of an ultra-stable optical cavity for space applications," Opt. Express **20**, 25409 (2012).
12. Z. Tai, L. Yan, Y. Zhang, X. Zhang, W. Guo, S. Zhang, and H. Jiang, "Transportable 1555-nm ultra-stable laser with sub-0.185-Hz linewidth," Chin. Phys. Lett. **34**, 090602 (2017).
13. N. Nemitz, T. Ohkubo, M. Takamto, I. Ushijima, M. Das, N. Ohmae, and H. Katori, "Frequency ratio of Yb and Sr clocks with 5×10^{-17} uncertainty at 150 seconds averaging time," Nat. Photonics **10**, 258 (2016).
14. L. Jin, Y. Jiang, Y. Yao, H. Yu, Z. Bi, and L. Ma, "Laser frequency instability of 2×10^{-16} by stabilizing to 30-cm-long Fabry-Pérot cavities at 578 nm," Opt. Express **26**, 18699 (2018).
15. D. G. Matei, T. Legero, S. Häfner, C. Grebing, R. Weyrich, W. Zhang, L. Sonderhouse, J. M. Robinson, J. Ye, F. Riehle, and U. Sterr, "1.5 μm lasers with sub-10 mHz linewidth," Phys. Rev. Lett. **118**, 263202 (2017).
16. W. Zhang, J. M. Robinson, L. Sonderhouse, E. Oelker, C. Benko, J. L. Hall, T. Legero, D. G. Matei, F. Riehle, U. Sterr, and J. Ye, "Ultrastable silicon cavity in a continuously operating closed-cycle cryostat at 4 K," Phys. Rev. Lett. **119**, 243601 (2017).
17. S. Häfner, S. Falke, C. Grebing, S. Vogt, T. Legero, M. Merimaa, C. Lisdat, and U. Sterr, "8×10^{-17} fractional laser frequency instability with a long room-temperature cavity," Opt. Lett. **40**, 2112 (2015).
18. K. Numata, A. Kemery, and J. Camp, "Thermal-noise limit in the frequency stabilization of lasers with rigid cavities," Phys. Rev. Lett. **93**, 250602 (2004).
19. M. A. Norcia, J. R. K. Cline, J. A. Muniz, J. M. Robinson, R. B. Hutson, A. Goban, G. E. Marti, J. Ye, and J. K. Thompson, "Frequency measurements of superradiance from the strontium clock transition," Phys. Rev. X **8**, 021036 (2018).
20. L. Jin, C. Hang, Y. Y. Jiang, C. J. Zhu, Z. Zheng, Y. Yao, G. X. Huang, and L. S. Ma, "Towards generation of millihertz-linewidth laser light with 10^{-18} frequency instability via four-wave mixing," Appl. Phys. Lett. **114**, 051104 (2019).
21. D. R. Leibrandt, M. J. Thorpe, M. Notcutt, R. E. Drullinger, T. Rosenband, and J. C. Bergquist, "Spherical reference cavities for frequency stabilization of lasers in non-laboratory environments," Opt. Express **19**, 3471 (2011).
22. S. Webster and P. Gill, "Force-insensitive optical cavity," Opt. Lett. **36**, 3572 (2011).
23. Q.-F. Chen, A. Nevsky, M. Cardace, S. Schiller, T. Legero, S. Häfner, A. Uhde, and U. Sterr, "A compact, robust, and transportable ultra-stable laser with a fractional frequency instability of 1×10^{-15}," Rev. Sci. Instrum. **85**, 113107 (2014).
24. X. Chen, Y. Jiang, B. Li, H. Yu, H. Jiang, T. Wang, Y. Yao, and L. Ma, "Laser frequency instability of 6×10^{-16} using 10-cm-long cavities on a cubic spacer," Chin. Opt. Lett. **18**, 030201 (2020).
25. J. Grotti, S. Koller, S. Vogt, S. Häfner, U. Sterr, Ch. Lisdat, H. Denker, C. Voigt, L. Timmen, A. Rolland, F. N. Baynes, H. S. Margolis, M. Zampaolo, P. Thoumany, M. Pizzocaro, B. Rauf, F. Bregolin, A. Tampellini, P. Barbieri, M. Zucco, G. A. Costanzo, C. Clivati, F. Levi,

and D. Calonico, "Geodesy and metrology with a transportable optical clock," Nat. Phys. **14**, 437 (2018).
26. M. Takamoto, I. Ushijima, N. Ohmae, T. Yahagi, K. Kokado, H. Shinkai, and H. Katori, "Test of general relativity by a pair of transportable optical lattice clocks," Nat. Photonics **14**, 411 (2020).
27. H. Chen, Y. Jiang, S. Fang, Z. Bi, and L. Ma, "Frequency stabilization of Nd:YAG lasers with a most probable linewidth of 0.6 Hz," J. Opt. Soc. Am. B **30**, 1546 (2013).
28. J. Luo, L.-S. Chen, H.-Z. Duan, Y.-T. Gong, S. Hu, J. Li, Q. Liu, J. Mei, V. Milyukov, M. Sazhin, C.-G. Shao, V. T. Toth, H.-B. Tu, Y. Wang, Y. Wang, H.-C. Yeh, M.-S. Zhan, Y. Zhang, V. Zharov, and Z.-B. Zhou, "TianQin: a space-borne gravitational wave detector," Class. Quantum Grav. **33**, 035010 (2016).
29. B. S. Sheard, G. Heinzel, K. Danzmann, D. A. Shaddock, W. M. Klipstein, and W. M. Folkner, "Intersatellite laser ranging instrument for the GRACE follow-on mission," J. Geodesy **86**, 1083 (2012).
30. Y. Luo, H. Li, and H.-C. Yeh, "Note: digital laser frequency auto-locking for inter-satellite laser ranging," Rev. Sci. Instrum. **87**, 056105 (2016).
31. F. Allard, I. Maksimovic, M. Abgrall, and Ph. Laurent, "Automatic system to control the operation of an extended cavity diode laser," Rev. Sci. Instrum. **75**, 54 (2004).
32. X. Guo, L. Zhang, J. Liu, L. Chen, L. Fan, G. Xu, T. Liu, R. Dong, and S. Zhang, "An automatic frequency stabilized laser with hertz-level linewidth," Opt. Laser Technol. **145**, 107498 (2022).
33. A. Didier, S. Ignatovich, E. Benkler, M. Okhapkin, and T. E. Mehlstäubler, "946-nm Nd:YAG digital-locked laser at 1.1×10^{-16} in 1 s and transfer-locked to a cryogenic silicon cavity," Opt. Lett. **44**, 1781 (2019).
34. L. S. Ma, P. Jungner, J. Ye, and J. L. Hall, "Delivering the same optical frequency at two places: accurate cancellation of phase noise introduced by an optical fiber or other time-varying path," Opt. Lett. **19**, 1777 (1994).
35. Y. Yao, Y. Jiang, H. Yu, Z. Bi, and L. Ma, "Optical frequency divider with division uncertainty at the 10^{-21} level," Natl. Sci. Rev. **3**, 463 (2016).
36. G. Yang, H. Shi, Y. Yao, H. Yu, Y. Jiang, A. Bartels, and L. Ma, "Long-term frequency-stabilized optical frequency comb based on a turnkey Ti:sapphire mode-locked laser," Chin. Opt. Lett. **19**, 121405 (2021).